Spectroscopic and Morphological Studies of Highly Conducting Ion-Implanted Rigid-Rod and Ladder Polymers

John A. Osaheni and Samson A. Jenekhe*

Department of Chemical Engineering, University of Rochester, Rochester, New York 14627-0166

Andrew Burns, Gang Du, Jinsoo Joo, Zhaohui Wang, and Arthur J. Epstein*

Department of Physics, Ohio State University, Columbus, Ohio 43210-1106

Chi-Shun Wang

University of Dayton Research Institute, Dayton, Ohio 45469

Received February 10, 1992; Revised Manuscript Received June 19, 1992

ABSTRACT: We report on the spectroscopic (UV–visible, IR, XPS, and Raman) characterization and morphological studies of $^{84}Kr^+$-implanted conducting rigid-rod and ladder polymers at a dose of 4×10^{16} ions/cm^2 and an energy of 200 keV. The rigid-rod polymers poly(*p*-phenylenebenzobis(thiazole)) (PBZT) and poly(*p*-phenylenebenzobis(oxazole)) (PBO), pseudo-ladder polymer poly((*p*-2,5-dihydroxyphenylene)-benzobis(thiazole)) (DPBT), and ladder polymer poly(benzimidazobenzophenanthroline) (BBL), all showed similar optical properties after implantation, namely, broad metallic absorption. XPS data of films revealed significant reduction in the heteroatoms and increased carbon content after implantation, which corroborates the observed insolubility of the implanted polymers even in the presence of Lewis acid–base coordination agents. The implanted samples were IR inactive, presumably due to symmetry and the small values or the absence of bond-dipole moments. However, the Raman spectrum of the implanted PBZT showed two principal bands with a drastic reduction in intensity and loss of the bands in the 1160–1300-cm^{-1} region compared to the Raman spectrum of the pristine polymer. PBO and BBL showed "brush-heap" morphologies after implantation, while the surface features of PBZT revealed a blistering effect of implantation. The morphology and electrical conductivity of the implanted materials were found to depend on the processing history of the pristine polymers. The room-temperature conductivity of these implanted rigid-rod and ladder polymers, typically ~80–200 S/cm, is significantly higher than that obtained to date by conventional doping techniques and was found to be remarkably stable even after annealing at temperatures up to 400 °C.

Introduction

Interest in highly conducting polymers has grown tremendously in the last decade because of their promising applications in various areas of technology.[1,2] Thus, great efforts have been made toward producing highly conducting polymers by chemical and electrochemical doping[3,4] of conjugated polymers and by ion implantation[5,6] of polymers.

Ion implantation as an approach to conducting polymers offers a number of advantages which are important in the fabrication of electronic devices: speed, homogeneity and reproducibility of the process, spatial selectivity, considerable latitude in the choice of "doping" atoms, and stability of the ion-implanted conducting materials.[5] However, one of the major drawbacks of ion implantation is that it is often difficult to determine the final molecular structure of the implanted polymer. In spite of this drawback, the advantages and potentials of modifying the structure, morphology, and desirable physical properties of polymers through ion implantation warrant a concerted effort toward the understanding of the structure and properties of these materials.

We are particularly interested in ion implantation studies of high-temperature polymers because the effects of pyrolysis which usually accompany implantation of organic polymers could be minimized in this class of polymers, if not completely eliminated. Thus, the effect of electronic and nuclear interactions of implanted ions on polymer structures and properties could be carefully and systematically studied. Accordingly, we chose to investigate the effect of $^{84}Kr^+$ implantation on the rigid-rod polymers poly(*p*-phenylenebenzobis(thiazole)) (PBZT) and poly(*p*-phenylenebenzobis(oxazole)) (PBO), the pseudoladder polymer poly((*p*-2,5-dihydroxyphenylene)-benzobis(thiazole)) (DPBT), and the ladder polymer poly(benzimidazobenzophenanthroline) (BBL). These polymers generally exhibit good mechanical and thermal properties.[7] However, efforts to dope some of them by conventional chemical and electrochemical doping techniques[4] have not yielded high conductivities that will be of major practical significance. To date, the highest conductivity of 200 S/cm reported[6a] for BBL, for example, was achieved through ion implantation with $^{40}Ar^+$ ions. This is about 2 orders of magnitude higher than that obtained by conventional doping techniques for BBL.[4] We have embarked on a study in order to understand, in a fundamental way, the effect of ion implantation on rigid-rod and ladder polymers. Our interests include understanding the nature of electrical conductivity, structure, and morphology of the implanted polymers and the optimum conditions for structure and physical property modifications in this class of polymers.

In this paper, we report on the use of various spectroscopic techniques, namely, UV–visible, infrared, X-ray photoelectron (XPS) and Raman spectroscopies, and Lewis acid coordination complexation, to study the effect of $^{84}Kr^+$ implantation on the molecular structure and electronic structure of PBZT, PBO, DPBT, and BBL, whose structures are shown in Chart I. We present the surface features and morphology of the implanted polymers revealed by scanning electron microscopy (SEM). The temperature-dependent dc conductivity of the im-

* To whom correspondence should be addressed.

0024-9297/92/2225-5828$03.00/0

Chart I

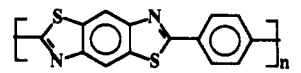

PBZT

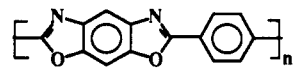

PBO

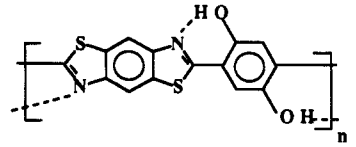

DPBT

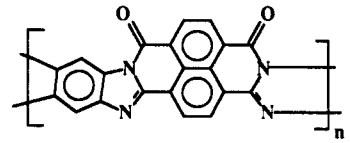

BBL

planted polymers and its stability with time and annealing temperature are also discussed.

Experimental Section

Samples of PBZT, PBO, DPBT, and BBL with intrinsic viscosities [η] of 16, 40, 14, and 9.8 dL/g, respectively, were supplied by the Polymer Branch of the Air Force Materials Laboratories (Dayton, OH) in the form of free standing films. We have also synthesized BBL with an intrinsic viscosity of 8.2 dL/g in our laboratory using the procedure reported in the literature.[8]

Thin films of the polymer (free standing and those supported on substrates) were also prepared for implantation and spectroscopic experiments. We used the method of reversible Lewis acid coordination complexation reported by Jenekhe et al.[9] to dissolve the rigid-rod and ladder polymers in nitromethane to obtain homogeneous solutions suitable for spin coating onto substrates. Thin films of PBZT, PBO, and BBL were spin-coated onto fused-silica substrates and also on 5-cm- × 5-cm-square glass for different postimplantation studies. The film thickness was controlled by preparing different solution concentrations as well as by adjusting the spinning speed. Typically, we used concentrations in the range 1–2 wt % polymer in $AlCl_3$/nitromethane and spinning speeds between 2000 and 3000 rpm. Film thicknesses were measured with an Alpha-Step (Tencor Instruments) profilometer which has a resolution of 1 nm. For purposes of obtaining optical absorption spectra before and after implantation, we prepared film thicknesses in the range 0.06–0.23 μm on fused-silica substrates. The thicknesses of the free standing films were measured with an electronic digital caliper and were between 25 and 300 μm.

Ion implantation was done at Honeywell Systems and Research Center (Bloomington, MN), using a Varian Model 400-AR ion implanter which has a maximum ion energy of 400 keV and a vacuum of 10^{-6} Torr. The entire set of polymers was implanted under identical conditions similar to those used previously,[6a] namely: $^{84}Kr^+$ ions with energies of 200 keV, fluences of 4×10^{16} ions/cm^2, and dose rates of 2 μA/cm^2. The samples were mounted on a sample stage cooled with water at room temperature (25–30 °C). Implantations were accompanied by faint glow and moderate to strong initial outgassing and an increase in chamber pressure. While PBZT, PBO, and BBL films glowed faintly with moderate outgassing, DPBT films were typically accompanied with strong initial outgassing. No analysis of the residual gas was done.

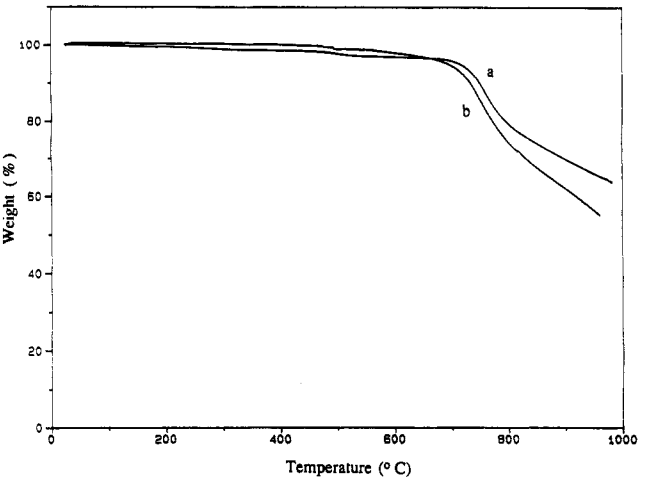

Figure 1. TGA thermogram of PBZT in N_2 (a) before and (b) after implantation.

Optical absorption spectra were recorded on Perkin-Elmer Models Lamda 9 and 19 UV–vis–near-IR spectrophotometers in the range 190–3200 nm. FTIR spectra were taken on free standing films by using Nicolet Model 2SXC and 60SX Fourier transform infrared (FTIR) spectrometers. X-ray photoelectron spectroscopy (XPS) was done on both free standing and spin-coated films using a Perkin-Elmer Physical Electronics Model 550 XPS system with a Mg Kα X-ray source (1253.6 eV). The X-ray power supply was operated at 15 kW and 10 mA. During all XPS or ESCA scans, the sample chamber pressure was kept below 1×10^{-8} Torr.

Raman spectra of the pristine and implanted polymers were taken with a Perkin-Elmer Model 1760-X FT-Raman spectrometer. The Raman spectra of the implanted samples were more difficult to acquire due to fluorescence and sample heating. Excitation at 1064 nm was afforded by a Quantronix Model 114 cw Nd:Yag laser. A conventional 180° back-scattering geometry was employed for the excitation and collection of the Raman scattered light. Laser powers at the samples were minimized by defocusing the beam, yielding a power at the sample of less than 50 mW. To reduce sample heating, each sample was bathed in liquid nitrogen boil-off. After the sample had cooled sufficiently, spectral artifacts associdated with sample heating, which is manifested as a "white" light continuum increasing in intensity toward larger wavenumbers, were reduced such that the Raman transitions of the sample could be observed.

Thermal analysis was done by using a Du Pont Thermal Analyst Model 2100 based on an IBM PS/2 Model 60 computer and equipped with a Model 951 thermogravimetric analyzer (TGA). The TGA runs were done in flowing nitrogen and at a heating rate of 10 °C/min. The implanted samples were also annealed for 20 mins at various temperatures in the range 50–400 °C in a vacuum oven and in a DSC cell to study the effect of heat treatment on the conductivity of the rigid-rod and ladder polymers. The same samples were used in each successive temperature treatment, starting at room temperature and progressing in 50-deg increments to 400 °C. After each heat treatment, the samples were allowed to cool down to room temperature before measuring the conductivity with the standard four-point probe technique, using a Keithley Model 220 current source and a Model 617 electrometer as a voltmeter.

Scanning electron microscopy (SEM) was done using a Stereoscan 200 (Cambridge Instrument) equipped with a Tracor Northern Model TN 5500 X-ray dispersive energy analyzer.

Results and Discussion

1. Molecular and Electronic Structures of Implanted Polymers. Thermogravimetric analysis (TGA) of the implanted materials shows the retention of high thermal stability. For example, implanted PBZT (see Figure 1) and BBL could withstand a temperature up to 720 °C in nitrogen without showing any weight loss, while implanted PBO was stable up to 680 °C and DPBT started

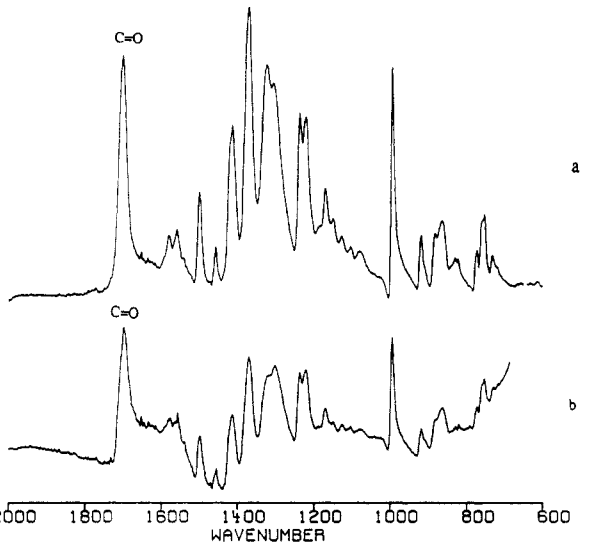

Figure 2. IR absorption spectra of a thick film (~25 μm) of BBL (a) before and (b) after surface implantation on one side.

to decompose at ~570 °C. Thus under the implantation conditions used in this study, the thermal properties of these polymers are retained in the implanted materials.

In order to get an indication of the effect of implantation on molecular structure from infrared spectra, thick free standing films (≥25 μm in thickness) implanted on one side only were examined. It should be noted that since the range of the ions in these materials is small (<1 μm) compared to the thickness (25 μm or more),[5,6] only a surface layer of the films is implanted. IR spectra of the thick films (25 μm thick) implanted on one side showed features similar to those of the unimplanted materials except that the intensities of the bands were reduced significantly. For example, the implanted BBL film showed only slight changes from the pristine material, as shown in Figure 2. The peak at 1323 cm^{-1} with a shoulder at 1305 cm^{-1} becomes broader after implantation with the main peak at 1303 cm^{-1} and a shoulder at 1322 cm^{-1}. This is the C—N stretching region of the spectrum. These differences are subtle and cannot account for the gross changes in the physical properties of implanted BBL. The intensity of the C=O band at ~1700 cm^{-1} in BBL is significantly reduced in the surface layer implanted film. One implication of the similarity between the IR spectra of the pristine and surface layer implanted materials is that the surface properties of these polymer films can be changed while the bulk properties are maintained. The surface structures might have become IR inactive due to symmetry, as a result of which all bond-dipole moments become small or absent. The IR spectra of the other free standing polymer films implanted on one side did not show any significant differences from the pristine materials except that the intensities of the various bands became weaker and slightly broader.

The XPS spectra of both pristine and implanted BBL for binding energies from −1000 to 0 eV are shown in Figure 3. The spectrum of the pristine polymer shows C 1s (~−287 eV), N 1s (~−402 eV), and O 1s (~−534 eV) in agreement with the reported data in the literature.[10] However, after implantation, there is significant reduction in the intensities of the peaks of the heteroatoms relative to the carbon peak. Although accurate chemical compositions cannot be calculated from the peak intensities because of the inherent limitations in using XPS to do elemental analysis, it can be observed that the N 1s peak has almost completely disappeared in the implanted spectrum while the O 1s is significantly reduced. The

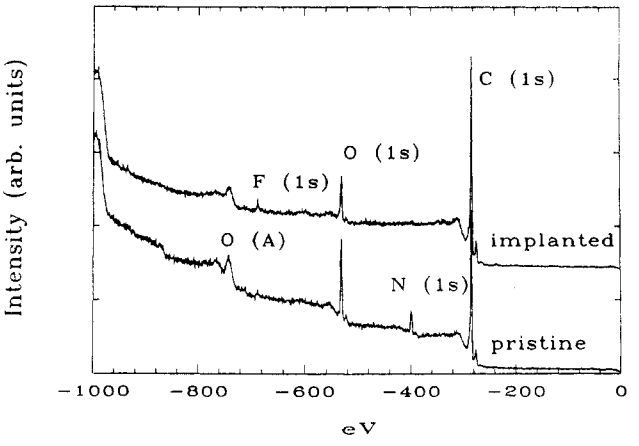

Figure 3. XPS spectra of pristine and implanted BBL.

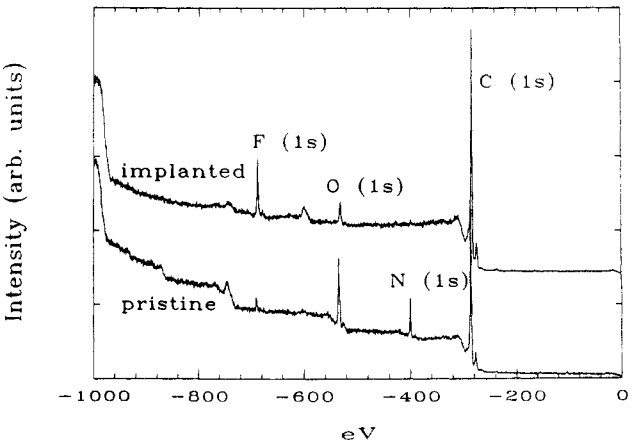

Figure 4. XPS spectra of pristine and implanted PBO.

drastic reduction of the heteroatoms can be traced to the electronic and nuclear interactions of the implanted ions with the atoms of BBL since degradation due to thermal heating of the samples is unlikely in these high-temperature polymers. The nitrogen sites appear to be the most susceptible to "attack" as seen ealier in the IR spectrum of BBL.

Figure 4 shows the XPS spectra for both the pristine and implanted PBO for binding energies from −1000 to 0 eV. As expected, the spectrum for the pristine polymer shows three principal peaks, namely, the C 1s, N 1s, and O 1s. After implantation, the N 1s peak disappears completely while the O 1s peak is drastically reduced. On the other hand, the intensity of the C 1s peak becomes stronger relative to the other peaks. There are also F 1s impurity peaks in both the pristine and the implanted samples, presumably scavenged from the poly(phosphoric acid) solvent used in the polymerization, as seen by Nalwa.[10]

In the light of the XPS and IR results which suggested the dramatic reduction of the heteroatoms, the solubility of the implanted free standing films was tested in the original solvent systems (Lewis acid/nitromethane) which were used in dissolving the pristine polymers. The implanted polymers were found to be insoluble. Insolubility of the implanted polymers shows that the molecular structures of the pristine polymers have been significantly changed. The possible changes in structure which might explain this insolubility include the following. (1) Elimination of the heteroatoms (N, S, O), as shown by the energy dispersive X-ray analysis (EDAX) and XPS data. The EDAX and XPS results indicated higher carbon content as well as depletion of heteroatoms in the implanted polymers compared with the pristine samples.

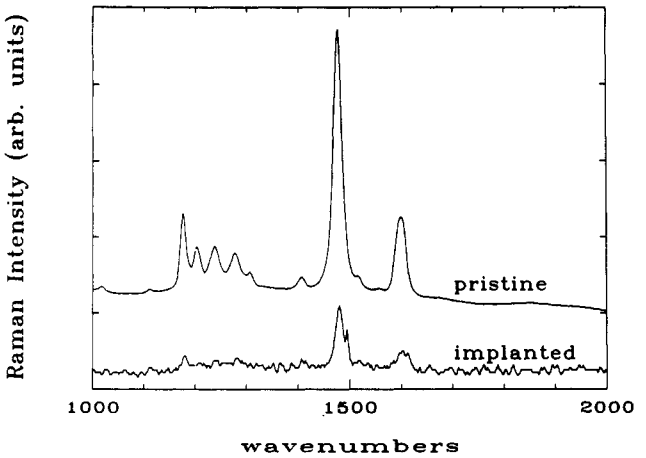

Figure 5. Raman spectra of pristine and implanted PBZT.

Since the solubility of these polymers in $AlCl_3$/nitromethane is due to $AlCl_3$ coordination to the heteroatom sites,[9] any significant reduction in the number of heteroatoms will cause insolubility of the polymers. The virtual elimination of the nitrogen sites and the drastic reduction of the other heteroatoms in the implanted polymers is in accord with the observed inability to solubilize the implanted polymers. This is in accord with implantation-induced carbonization. The unimplanted side of the polymers remained soluble in Lewis acid/nitromethane systems. (2) Another possible reason for insolubility is that ion implantation can induce chain cross-linking. It is possible that cross-linking might be induced if reactive species such as free radicals are generated during implantation. In any case, this insolubility of the implanted rigid-rod and ladder polymers can be exploited as a way of obtaining thin films of conducting implanted polymer layers in that the unimplanted areas can be etched away with the usual solvents for the polymer. Selective implantation and etching suggest the possible applications of these high-temperature polymers in microelectronic devices.[6a]

The Raman spectra of the pristine and implanted PBZT are shown in Figure 5. As stated earlier in the Experimental Section, the implanted polymer showed excessive fluorescence and sample heating. The Raman transitions are found in the 1700–1000-cm^{-1} shift region; hence Figure 5 has been plotted from 2000 to 1000 cm^{-1}. Apparent transitions occurring in the lower (1000–500-cm^{-1}) shift region and higher wavenumbers (3200–2000 cm^{-1}) are due to Rayleigh filter response to the sample's fluorescence and residual heating, respectively. The Raman spectrum of the pristine PBZT shows two main bands at 1600 and 1480 cm^{-1} and several medium bands in the 1160–1300-cm^{-1} shift region, consistent with what is reported in the literature.[11b] However, the spectrum of implanted PBZT shows only two Raman bands, one intense band at 1480 cm^{-1} with a shoulder at ~1500 cm^{-1} and a band of medium intensity at 1600 cm^{-1}. This Raman spectrum in conjuction with the XPS results provides a useful means of elucidating the structural changes that occur as a result of the implantation.

From group frequency analysis, the strong bands in the 1100–1600-cm^{-1} region of the Raman spectrum are likely assignable to the stretching vibration of the central heterocyclic group, the phenyl ring, and the C—C bond linking them.[11] The band at 1600 cm^{-1} has been assigned to the phenyl ring stetching on the basis of model compound studies,[11] while the origin of the band at 1480 cm^{-1} has not been unequivocally explained. The strong interaction between the C=N and C=C stretching

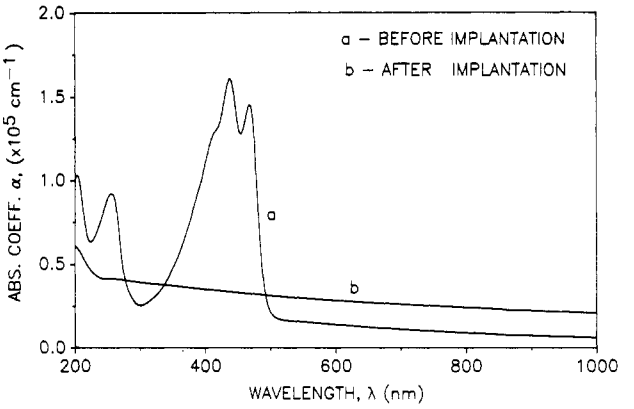

Figure 6. Electronic absorption spectra of PBZT (a) before and (b) after implantation.

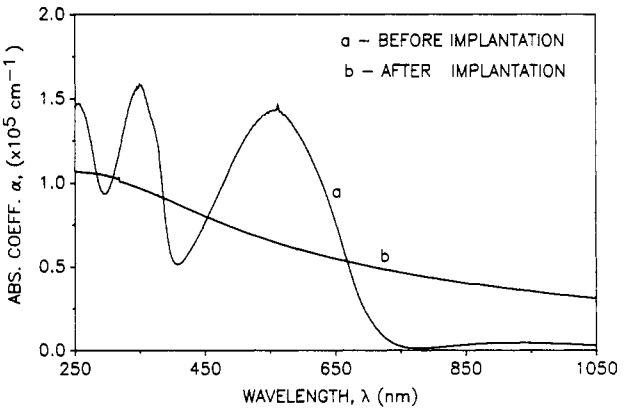

Figure 7. Electronic absorption spectra of BBL (a) before and (b) after implantation.

vibrations in the heterocyclic ring results in the overlap of the Raman bands so that they completely lose their individual identity. Considering the XPS results, one can argue that the band at 1480 cm^{-1} in the implanted sample is likely due to C=C stretching vibration since the heteroatoms have been significantly reduced or eliminated. The reason for the observed split in this band is not clear but it thus suggests that there are probably other kinds of residual carbon–carbon or carbon–heteroatom linkages contributing to this band.

The Raman spectrum of the implanted PBZT shows a significant difference from that of the protonated PBZT in methanesulfonic acid (MSA) solution.[11b] While the protonated sample shows intense bands at 1218 and 1295 cm^{-1}, the implanted polymer does not show any band in this region. Protonation of PBZT has been proposed to occur principally at the heterocyclic segment, specifically on the nitrogen atoms.[11b] Intuitively, we do not expect to see any Raman bands associated with any kind of interactions with the nitrogen atoms in the implanted material since the XPS results show virtual elimination of the heteroatoms. The ratio of the intensity of the band at 1480 cm^{-1} to the band at 1600 cm^{-1} is essentially constant in the implanted and pristine polymer unlike the protonated PBZT where the intensity of the band at ~1600 cm^{-1} increases dramatically in MSA solution due to a reduction in the twist angle of the phenyl rings.[11b] Changes in the chain conformation are not expected to occur readily in the solid state as a result of implantation; hence the relative intensity of the bands at 1600 and 1480 cm^{-1} remains constant in the implanted and pristine PBZT.

Figures 6 and 7 show the electronic absorption spectra of PBZT and BBL thin films, respectively, before and after implantation with $^{84}Kr^{+}$ ions. It is seen that after implantation, the polymer absorption bands in the visible

disappear and are replaced by a finite absorption extending from the infrared through the visible and becoming broader in the UV. These electronic absorption spectra of the implanted polymers are characteristic of disordered metals.[12] This interpretation has been corroborated by temperature-dependent conductivity, thermopower, microwave conductivity, and magnetoresistance measurements which indicated that the implanted polymers are disordered metals.[13] Prior to implantation, PBZT and PBO thin films are yellow while the BBL thin film is purple in transmission with metallic luster in reflection. After implantation, all three polymer thin films became "metallic" in color yet quite transparent to visible light. The appearance of a broad absorption band in the visible after implantation has been reported for poly(diacetylene)[14] at a fluence greater than 10^{14} ions/cm^2. In the latter, the optical density of the implanted material in the visible was greater than that of the pristine poly(diacetylene). For implanted PBZT, PBO, and BBL, the strong interband transition in the pristine polymers is replaced by a broad featureless absorption (extending from the IR to the UV) after ion implantation with a fluence of 4×10^{16} ions/cm^2 or greater. Notice from Figures 6 and 7 that the absorption coefficient of the implanted polymers is less than that of the pristine materials in the visible.

Film thickness measurement after implantation of samples spin-coated on silica substrates revealed that the implanted materials were slightly thinner and more dense than the pristine films. A reduction of up to 15% of the thickness was observed in PBO films, and the films were much more difficult to scratch off from the substrates after implantation, whereas the unimplanted materials were quite flexible and peel-off easily from the substrates.

Overall, these spectroscopic results that include electronic, FTIR, FT-Raman, and XPS spectra clearly indicate that the dramatic changes in molecular and electronic structures, after implantation, are consistent with substantial graphitization or carbonization of the implanted layers. Our studies of the bulk surface morphology and electrical properties of the implanted rigid-rod and ladder polymers, which are discussed below, also support the conclusion of substantial graphitization of implanted layers.

2. Morphology of Implanted Polymers. As a way of observing the effect of ion implantation on the morphology of free standing films of PBZT, PBO, DPBT, and BBL, we took SEM pictures of both the pristine and implanted polymers. While retaining high thermal stability and good mechanical integrity, the implanted polymers have surface features and morphology which are completely different from the pristine materials, as would be expected.

Parts a and b of Figure 8 show the surface features of the implanted and pristine areas of oriented and unoriented DPBT, respectively. In Figure 8a, the unimplanted region is essentially featureless while the implanted region shows features which suggest a porous microstructure and "fibrillar" morphology. The pore structures are oriented transverse to the stretch direction. In Figure 8b the unoriented sample shows porous features with nonintersecting pores on the surface of the implanted polymer. Comparing Figure 8a,b at the same magnification level, it is seen that the morphology of the implanted region depends on the processing history of the polymer prior to implantation. The stretch-oriented samples show noninterconnecting pores. Although this is true for the unoriented samples, it is clear that the length and width of these pores are larger in the oriented samples. A typical pore size of the order of 2 μm $\times$ 0.4 μm dominates the surface of the stretched-oriented samples of DPBT (Figure 8a).

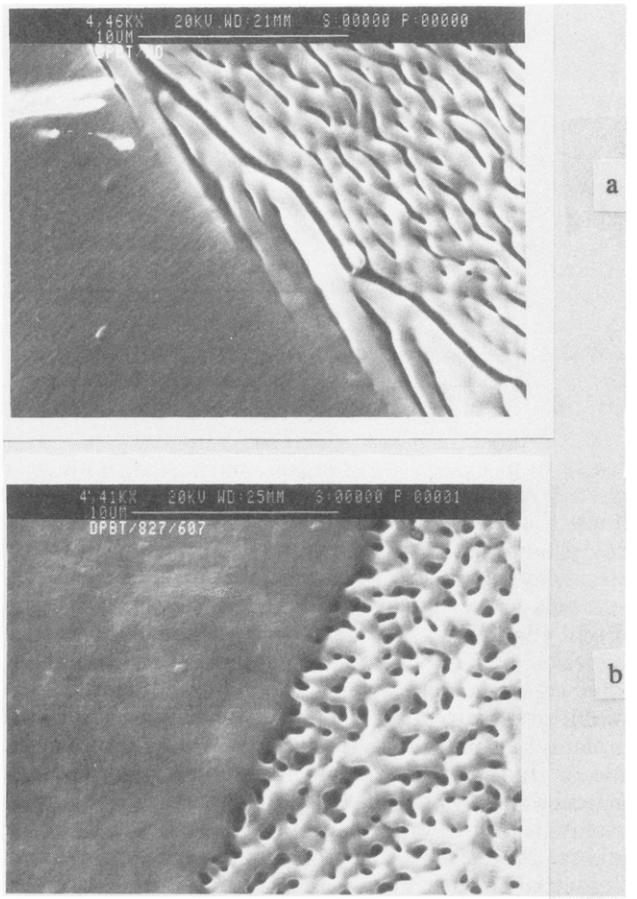

Figure 8. SEM pictures of implanted and pristine areas of (a) stretched-oriented and (b) unoriented DPBT films.

Figure 9 shows the SEM pictures of both pristine (9a) and implanted (9b) BBL at the same magnification. It is seen that the implanted surface exhibits "brush-heap" morphology. Similar brush-heap features are seen on the surface of implanted PBO, as shown in Figure 10. Although the morphologies of the pristine BBL and PBO are somewhat different, it is interesting to see that, after implantation, both polymers show similar features, suggesting that the natures of the ion beam interactions with the surface layer of the materials are similar. The blistering effect of ion implantation is revealed on the surface of implanted PBZT, as shown in Figure 11. The pristine surface of PBZT is featureless whereas, after implantation, the surface has blisters at isolated spots on the surface.

In polymers, most of the damage produced by high-energy ion implantation is actually caused by secondary electrons that are generated along the primary ion track.[15] By virtue of the low energies of these electrons, they do not travel far from their primary track but can cause numerous additional ionization events, leading to ion and free radical formation, chain scission, and cross-linking. Reactive species such as free radicals can diffuse away from the incident track and react with the polymer. The nature of the damage shown by SEM implies that the diffusion of the reactive species in DPBT occurred more in the lateral direction (a few microns) compared with the cases of the other polymer samples. The diffusion of the evolved gases and reactive species out of BBL, PBO, and PBZT surfaces must have occurred in the direction perpendicular to the surface of the films rather than in the lateral direction.

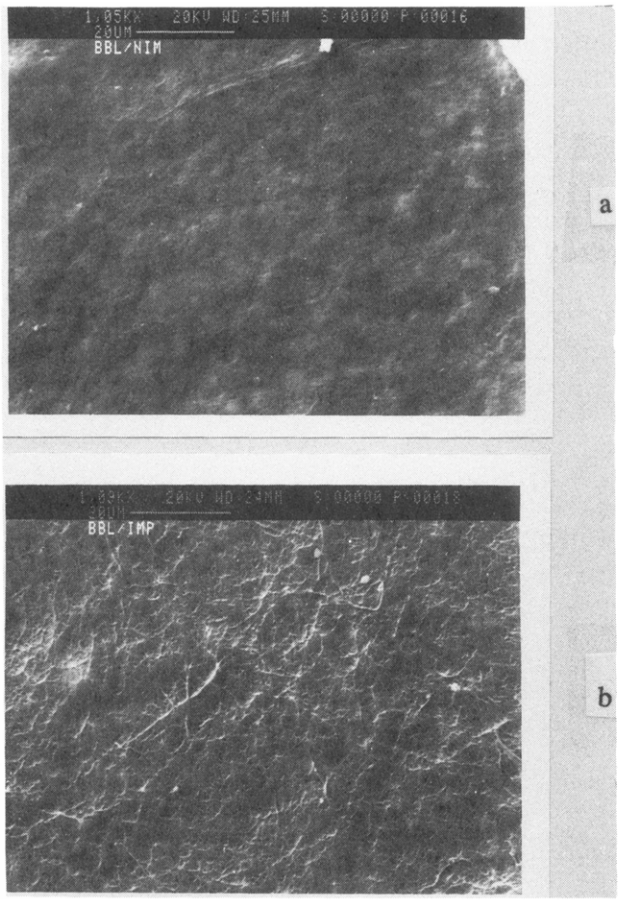

Figure 9. SEM pictures of (a) unimplanted and (b) implanted BBL films.

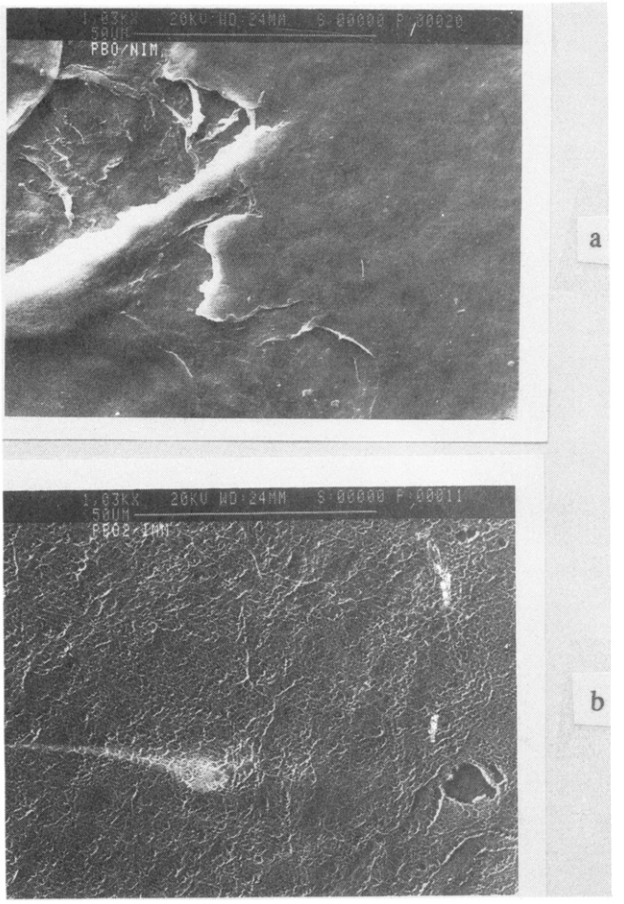

Figure 10. SEM pictures of (a) unimplanted and (b) implanted PBO films.

3. Electrical Conductivity of Implanted Polymers. A detailed study of the electrical properties which include a theoretical model for the temperature-dependent dc conductivity, magnetoresistance, and thermopower will be reported elsewhere.[13] Here we briefly mention that the electrical conductivities of the implanted rigid-rod and ladder polymers determined by the standard four-point probe techniques were found to be about 2 orders of magnitude higher than those obtained by conventional doping techniques.[4] Also, we have found that the electrical properties of the implanted materials, as with their spectroscopic properties, do not change with time for over a 1-year period. Figure 12 shows the dc conductivity of implanted unoriented PBO film from 4 to 300 K. It is seen that within this temperature range, the conductivity slowly increases from 50 S/cm at 4 K to 80 S/cm at 300 K (a factor of 1.6). The weak temperature dependence is reminiscent of a disordered metal. The implanted stretched-oriented PBO samples had a room-temperature conductivity σ_{RT} of 160 S/cm. Thus, the conductivity of implanted PBO films is enhanced by a factor of 2 by stretch orientation of the pristine polymer.

Table I shows the measured room-temperature conductivity of the annealed (σ_a) sample normalized with the conductivity of the unannealed sample (σ_{ua}). The measured conductivities of the heat-treated implanted samples were found to be essentially the same as the unannealed samples over the entire range of annealing temperatures, 50–400 °C, as exemplified in Figure 13 for the conductivity of implanted PBO. The slight variations are within experimental errors. This observation is in sharp contrast to the reported[16] heat-treated implanted DPBI, DPBO, DPBT, and BBL that showed approximately 3 orders of magnitude decrease in the conductivity after annealing at 400 °C for 40 min. It must be emphasized, however, that the implantation conditions used in the latter (190-keV energy, 0.1 μA/cm^2 beam current) is different from the ones used here which might influence the nature of the interactions of the Kr^+ ions with the substrate. The beam intensity used here is a factor of 20 greater that the ones used in earlier studies,[16] which might be the reason for the ready release of the Kr^+ ions when annealed at high temperatures. The conditions used in this study result in a more drastic and stable change in the structure, morphology, and physical properties of these rigid-rod and ladder polymers. This observed stability of the physical properties (mechanical, thermal, and electrical conductivity) with temperature and time is an important factor in the utilization of the implanted materials in various technological applications.

Conclusions

The effects of ion implantation on the molecular and electronic structures of rigid-rod and ladder polymers have been studied with various spectroscopic techniques, and the surface features and morphologies have been investigated with scanning electron microscopy. Our results showed that while this class of polymers retains its thermal and mechanical integrity after implantation, the molecular and electronic structures as well as the morphology have been significantly changed. The implanted polymers exhibit broad metallic absorption with absorption coefficients lower than that of the pristine materials in the UV–visible region. The inability to solubilize the implanted polymers using Lewis acid–base coordination complexation coupled with the XPS, EDAX, and FTIR data confirm that the major change in the molecular

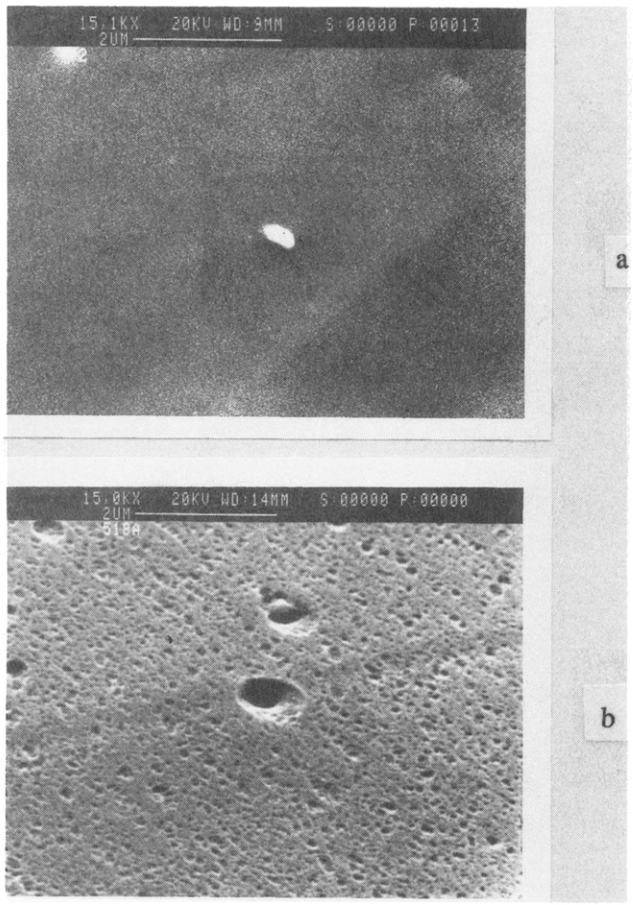

Figure 11. SEM pictures of (a) unimplanted and (b) implanted PBZT films.

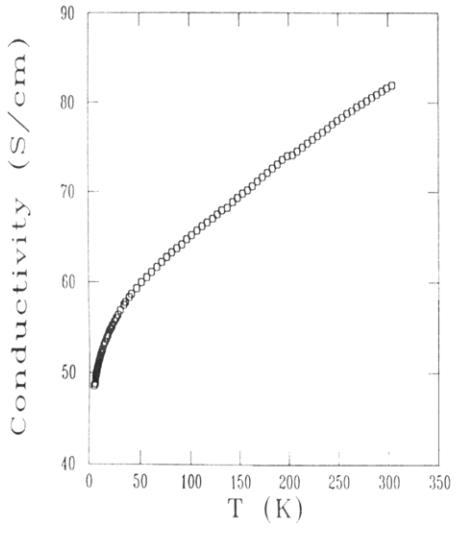

Figure 12. Temperature-dependent dc conductivity of $^{84}Kr^{+}$-implanted PBO at 4×10^{16} ions/cm^2.

structure is the reduction or virtual elimination of the heteroatoms, resulting in substantial carbonization of the polymers. The Raman spectrum of the implanted PBZT suggests that the effect of implantation is completely different from the effect of protonation. Although the Raman spectrum of protonated PBZT showed new and more intense bands in the 1160–1300-cm^{-1} shift region, the implanted sample reported here showed loss of the bands in this region as a result of structural modification. The morphology of the implanted layers was typically brush-heap and was found to depend on the processing history prior to implantation. Heat treatment of the

Table I
Effect of Annealing Temperature on the Conductivity of Implanted PBO, PBZT, and BBL

	normalized conductivity[a] $(\sigma_a/\sigma_{ua})_{RT}$		
T (°C)	PBO	PBZT	BBL
~27	1.00	1.00	1.00
50	0.98	0.97	1.02
100	1.04	1.18	0.96
150	0.94	0.98	0.91
200	1.07	1.10	0.90
250	1.06	1.19	1.08
300	1.08	1.19	1.15
400	1.17	1.20	0.92

[a] Conductivity of the annealed (σ_a) normalized with the conductivity of the unannealed (σ_{ua}) sample at room temperature.

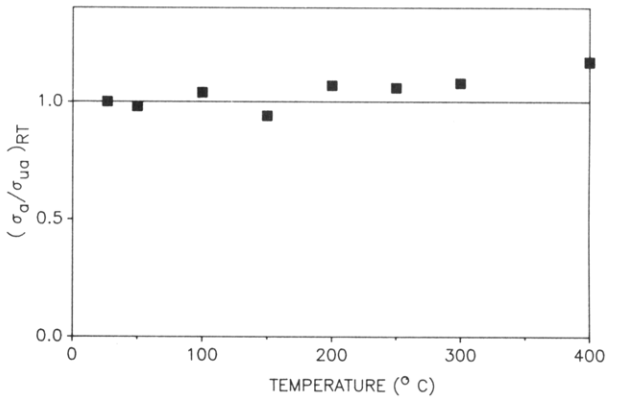

Figure 13. Effect of annealing temperature on the room-temperature conductivity of the $^{84}Kr^{+}$-implanted PBO of Figure 12.

implanted rigid-rod and ladder polymers showed that the conductivity of about 80–200 S/cm imparted by implantation under the present conditions, namely, 200-keV energy, 2 μA/cm^2 beam current, and 4×10^{16} ions/cm^2 dose, is very stable with time and temperature. The weak temperature-dependent dc conductivity of the implanted polymers is reminiscent of disordered metals.

Acknowledgment. We thank Jerry Burkett for the polymer synthesis scale-up, Stan Tibbetts of Honeywell Inc. for the implantations, Roy Tucker for his technical assistance in the XPS work, Dr. André J. Sommer for the FT-Raman spectra and Dr. Richard P. McCall for various discussions. This work was supported in part by the Air Force Office of Scientific Research.

References and Notes

(1) (a) Brédas, J. L., Chance, R. R., Eds. *Conjugated Polymeric Materials: Opportunities in Electronics, Optoelectronics, and Molecular Electronics*; Kluwer Academic Publishers: Dordrecht, Holland, 1990. (b) Skotheim, T. A., Ed. *Handbook of Conducting Polymers*; Marcel Dekker; New York, 1986. (c) See, for examples: *Synth. Met.* **1991**, *41–43* (Proceedings of the International Conference on Science and Technology of Synthetic Metals, Tubingen, Germany, Sept 2–9, 1990). *Synth. Met.* **1989**, *27–29* (Proceedings of the International Conference on Science and Technology of Synthetic Metals, Santa Fe, NM, June 25–July 2, 1987).

(2) Frommer, J. E.; Chance, R. R. *Encyclopedia of Polymer Science and Engineering*; John Wiley, New York, 1986; p 462.

(3) (a) MacDiarmid, A. G.; Somasiri, N. L. O.; Salaneck, W. R.; Lundstrom, I.; Liedberg, B.; Hasan, M. A.; Erlandsson, R.; Konrasson, P. *Springer series, in Solid Sate Sciences*; Springer: Berlin, 1985; Vol. 63, p 218. (b) MacDiarmid, A. G.; Epstein, A. J. *Faraday Discuss. Chem. Soc.* **1989**, *88*, 317.

(4) (a) Jenekhe, S. A. *Polym. Mater. Sci. Eng.* **1989**, *60*, 419. (b) Kim, O.-K. *J. Polym. Sci., Polym. Lett. Ed.* **1982**, *20*, 663. (c) Kim, O.-K. *Mol. Cryst. Liq. Cryst.* **1984**, *105*, 161.

(5) Jenekhe, S. A. *Encyclopedia of Polymer Science and Engineering*, 2nd ed.; John Wiley: New York, 1989; Suppl. Vol., p 352.
(6) (a) Jenekhe, S. A.; Tibbetts, S. J. *J. Polym. Sci., Part B: Polym. Phys. Ed.* **1988**, *26*, 201. (b) Dresselhaus, M. S.; Wasserman, B.; Wnek, G. E. In *Ion Implantation and Ion Beam Processing*; Hubler, G. K., Holland, O. W., Clayton, C. R., White, C. W., Eds.; Materials Research Society: Pittsburgh, PA, 1984; Vol. 27, pp 413–422.
(7) Arnold, F. E.; Van Deusen, R. L. *J. Appl. Polym. Sci.* **1971**, *15*, 2035.
(8) (a) Arnold, F. E.; Van Deusen, R. L. *Macromolecules* **1969**, *2*, 497. (b) Wolfe, J. F. *Polym. Mater. Sci. Eng.* **1986**, *54*, 99.
(9) (a) Jenekhe, S. A.; Johnson, P. O. *Macromolecules* **1990**, *23*, 4419. (b) Jenekhe, S. A.; Johnson, P. O.; Agrawal, A. K. *Macromolecules* **1989**, *22*, 3216.
(10) Nalwa, H. S. *Polymer* **1991**, *32*, 802.
(11) (a) Venkatesh, G. M.; Shen, D. Y.; Hsu, S. L. *J. Polym. Sci., Polym. Phys. Ed.* **1981**, *19*, 1475. (b) Shen, D. Y.; Venkatesh, G. M.; Burchell, D. J.; Shu, P. H. C.; Hsu, S. *J. Polym. Sci., Polym. Phys. Ed.* **1982**, *20*, 509.
(12) Schmid, E. D.; Brosa, B. *J. Chem. Phys.* **1972**, *56*, 6267.
(13) (a) Wang, Z. H.; Burns, A.; Du, G.; Joo, J. S.; Epstein, A. J.; Osaheni, J. A.; Jenekhe, S. A.; Wang, C. S. Submitted for publication. (b) Burns, A.; Wang, Z. H.; Joo, J.; Epstein, A. J.; Osaheni, J. A.; Jenekhe, S. A.; Wang, C. S. *Mater. Res. Soc. Proc.* **1992**, *247*, 735.
(14) Elman, B. S.; Blackburn, G. F.; Thakur, M. K.; Sandman, D. J.; Samuelson, L. A.; Kenneson., D. G. *Nucl. Instrum. Methods Phys. Res. B* **1987**, *19/20*, 872.
(15) Makhlis, F. A. *Radiation Physics and Chemistry of Polymers*; John Wiley: New York, 1975.
(16) Wang, C. S.; Burkett, J.; Lee, C. Y. C.; Arnold, F. E. *Polym. Mater. Sci. Eng.* **1991**, *64*, 171.

Registry No. PBZT (SRU), 69794-31-6; PBO (SRU), 60871-72-9; DPBT (SRU), 121595-27-5; BBL (SRU), 34398-57-7; ^{84}Kr, 14993-91-0.